JOURNAL OF APPLIED ELECTROCHEMISTRY 15 (1985) 711–717

The dissolution of iron from the negative material in pocket plate nickel–cadmium batteries

M. Z. A. MUNSHI*, A. C. C. TSEUNG

Department of Chemistry, The City University, Northampton Square, London EC1 0HB, UK

J. PARKER

Marathon-Alcad Limited, PO Box 4, Union Street, Redditch Worcestershire B98 7BW, UK

Received 12 July 1984; revised 3 October 1984

A common mode of failure of nickel–cadmium flooded pocket plate cells is iron poisoning of the positive plate due to transfer of iron into the active material from active materials and materials of construction. Nickel plated steel pockets are sometimes used to minimize iron dissolution, particularly on the positive electrode. Sometimes α-Fe_2O_3 is used as an additive to the cadmium electrode. This paper assesses the extent of dissolution of iron from α-Fe_2O_3 by using electron microscopy, X-ray crystallography, cyclic voltammetry, coulometric and atomic absorption measurements.

1. Introduction

In industrial nickel–cadmium pocket plate flooded cells, it is standard practice for the negative active material to contain iron or an iron oxide to prevent crystal growth of the cadmium and thus prevent reduction in capacity of the negative plate with cycling. A common mode of failure of these cells is the poisoning of the positive active material by iron compounds. Previous work [1] has shown that the main part of the iron transferred to the positive active material originates from the perforated steel strips containing the active material. Iron may also arise from the steel strip containing the negative active material; the potential of this strip is in the corrosion region indicated by the Pourbaix diagrams.

It has been demonstrated [2] that the corrosion can be reduced by nickel plating of the negative steel strip. However, it is possible that some transfer of iron from the Fe_2O_3, if this is used as an additive in the negative active material, may also take place.

Fig. 1 shows that iron at high pH values is in the passive region at potentials above -0.400 V vs the standard hydrogen electrode (SHE). In alkaline media, iron demonstrates considerable stability due to the formation of a passive oxide film which affords protection. When connected to high surface area cadmium, as in the case of a negative plate, the potential of iron is maintained in the active potential region of -0.809 V (i.e. where corrosion can occur). The degree of corrosion will depend on how easily any protective oxide present is reduced to bare metal.

Consideration of the potential–pH diagram for iron (Fig. 1) [3] indicates that iron in cell electrolyte at a potential of about -0.809 V (i.e. that of the cadmium on open-circuit) is unstable and will corrode, forming a soluble iron ion, $HFeO_2^-$. Salkind *et al.* [4] have also stated that at this potential iron has a tendency to corrode at a much faster rate in the presence of cadmium. However, when the additive involved is α-Fe_2O_3, at potentials more negative than -0.877 V, it is possible that some of the active α-Fe_2O_3 could become reduced to elementary iron via the $HFeO_2^-$ complex. This potential is exceeded during the overcharge of cadmium electrodes. As the potential–pH diagram of Fig. 2 shows,

**Present address*: Department of Metallurgy and Materials Science, McMaster University, Hamilton, Ontario, Canada L8S 4L7.

0021–891X/85 $03.00 + .12 © 1985 Chapman and Hall Ltd.

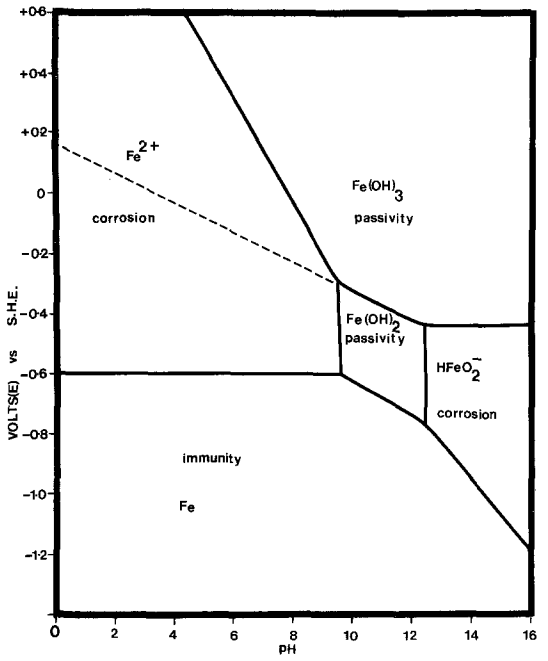

Fig. 1. Potential-pH diagram for $Fe/Fe(OH)_2/Fe(OH)_3/H_2O$ system at 25° C.

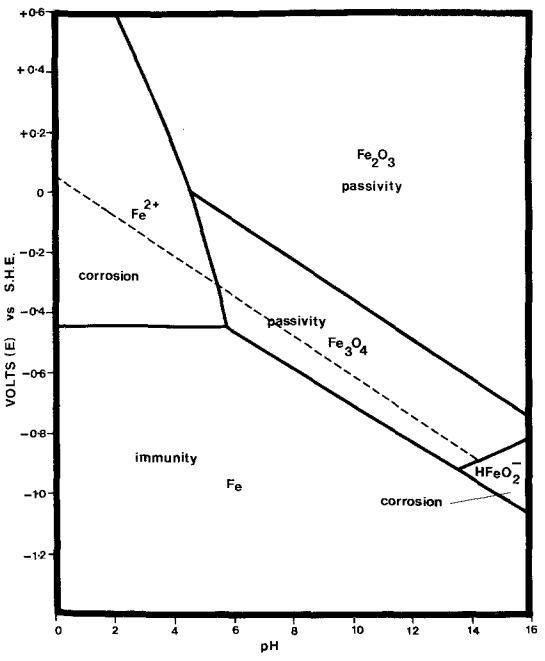

Fig. 2. Potential–pH diagram for $Fe/Fe_2O_3/Fe_3O_4/H_2O$ system at 25° C.

there is a region in the $Fe/Fe_2O_3/Fe_3O_4$ system at pH 14 in which $HFeO_2^-$ is present and the iron oxide has to pass through this intermediate phase before reduction to iron.

Ojefors [5], using cyclic voltammetry has shown with sintered iron electrodes that iron exhibits a distinct corrosion region over the potential range -0.90 to -0.65 V.

The fact that iron has a detrimental effect on the capacity of the positive plate has been shown by Salkind and Falk [6]. Tichenor [7] noted that ferric hydroxide additions to the nickel hydroxide decreased the electrode capacity. The effects were attributed to growth of insulating barrier layers of one form or another thereby limiting electronic conduction processes.

Tuomi [8] concluded that since ferric hydroxide has a lower oxygen evolution potential than the potential required to oxidize the positive active material fully, there will be a loss in capacity. This effect will be more pronounced if the ferric hydroxide is uniformly distributed in the positive plate and the total amount of iron incorporated in the positive plate may not be as important as the degree of dispersion in the positive plate. Experimental work by Parker [9] confirmed that this was indeed the case: tests carried out on two sets of Ni–Cd cells containing 0.4% and 1.0% iron in the positive plate gave 100% of the theoretical capactiy. However, another set of cells containing only 0.4% of iron in the positive plates, gave only 64% of the theoretical capacity. Unfortunately, no detailed examination was made of the iron distribution in the two sets of cells.

Although it has been shown that the poisoning of the positive plate is due mainly to iron corrosion of the cell components and consequent incorporation into the positive active material, it is believed that there could be a small contribution towards the iron-deposits from the dissolution of the iron oxide in the negative active material.

The main purpose of this paper is to present experimental evidence supporting this assumption.

2. Experimental details

Cycling tests were carried out on a single pocket electrode in 4.5 M KOH and any dissolved species were electroplated onto a pure nickel counter electrode and examined under an electron microscope using EDAX, X-ray diffraction and

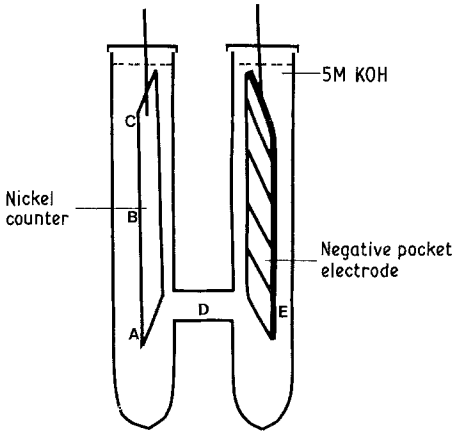

Fig. 3. Experimental cell.

cyclic voltammetry. The amounts of iron deposited were measured by coulometric measurements.

The experimental cell used for cycling is shown in Fig. 3. The negative electrode mixture had the following composition:

β-$Cd(OH)_2$	48%
α-Fe_2O_3	48%
graphite	4%

The mixture was enclosed in a pocket made from a thin perforated pure nickel ribbon and its characteristics were as follows:

theoretical capacity	0.696 A h
width	1.2 cm
height	5.5 cm
overall thickness	3.2 cm
weight of active material	2.5 g

The counter electrode consisted of a thin perforated pure nickel ribbon, 5.5 x 1.2 cm^2 in dimension, the distance between the working negative electrode and the counter electrode being 3 cm. Physical agitation was carefully avoided and electrochemical agitation was minimized by using a low current and also by switching the circuit off at the onset of gas evolution from the cadmium electrode.

The electrolyte was made from BDH Aristar KOH, and the specific gravity of the electrolyte was adjusted to 1.200. The iron content of the electrolyte was determined by atomic absorption spectrophotometry to be 1.4 ppm. A Chemical Electronics Potentionstat was used in the galvanostatic mode for charging and discharging of the electrode. The negative electrode was first subjected to eight forming charge–discharge cycles in the following manner:

1st four cycles; charge at $c/10$ rate for 14 h, discharge at $c/10$ rate to -0.0700 V vs Hg/HgO reference electrode.

2nd four cycles; charge at $c/5$ rate for 7 h, discharge at $c/5$ rate to -0.700 V vs Hg/HgO reference electrode.

This lengthy formation procedure was adopted to ensure that there was no further visible shedding of the active material from the cadmium electrode. The cycling operations were carried out in a separate cell. After each cycle the electrode was washed using deionized distilled water and fresh electrolyte was added to the cell. The negative electrode was then charged in this cell. Following charging, the negative electrode was transferred to a test cell where it underwent anodic oxidation at the $c/10$ rate to -0.0700 V vs Hg/HgO reference electrode using a pure nickel perforated foil as the counter electrode. This charge–discharge procedure in separate cells was carried out to prevent any removal of electrodeposited material from the nickel ribbon in the test cell during charging of the negative and was repeated fifteen times at room temperature.

Coulometric studies were performed on the counter nickel electrodes and the discharges were conducted at a constant current of 1 mA. The voltage of the nickel electrodes were measured with reference to a standard Hg/HgO electrode and the electrolysis terminated at a point when the voltage varied no more.

The polarization curves on the nickel electrode were measured under cyclic voltammetric conditions using the Chemical Electronics 0.5 A–2 V Potentiostat in conjunction with a sweep generator a J.J. PL4 recorder. All solutions were deaerated by bubbling with N_2 before each experiment.

EDAX photographs were taken on the nickel counter electrode from the test cell at the A, B and C position at a magnification of 300x. The electron beam of the electron microscope was generated at 40 kV and a high resolution setting was used. The scans were carried out on a 10 eV/Channel for 520 s time interval.

X-ray powder diffraction measurements were also carried out on the active material in the charged and discharged state. The samples were

examined on a Phillips P.W. 1010 X-ray diffractometer using the $K\alpha$ radiation of molybdenum. The patterns were taken from a ground mixture of the active material and the scanning speed on the goniometer was kept at $1/8^\circ$ min^{-1} for the 2θ angle with corresponding paper speed. In addition to the above examination on the nickel cathode deposits, atomic absorption analysis of the solution was carried out on a Perkin Elmer 370 type spectrophotometer.

In order to measure the relative participation of the α-Fe_2O_3 additive and mild steel pockets normally used to contain the active material in a pocket cadmium electrode the experiments were repeated using a thin perforated unplated mild steel ribbon in place of the nickel ribbon to make the negative electrode. The amount of iron transferred was compared with that from the pure nickel ribbon electrode under the same experimental conditions.

3. Results and discussion

3.1. *EDAX and coulometric studies*

Figs 4–6 show the distribution of iron along the electrode. Fig. 7 shows a scan on unused nickel which did not show any iron to be present. The iron $K\alpha$ signal appears at 623 eV, the nickel $K\alpha$, $K\beta$ at 7060 and 7800 respectively and the potassium $K\alpha$ from the caustic solution at 3312 eV. The cadmium signal occurs at 3313 eV and careful examination on the microscope eliminated any question of cadmium being present and the line in that region was due to the potassium $K\alpha$. The scans showed that iron was not present on unused nickel, but present in increasing quantities on the treated nickel from positions near the cell bridge, i.e. position A. EDAX is essentially a qualitative technique. The actual quantity of iron deposited was determined coulometrically from a potential time curve obtained on charge and discharge of the nickel electrode. This is shown in Fig. 8 together with the curve obtained on the unused nickel ribbon. Both curves were obtained at a constant current of 1 mA and it is seen that the electrodeposited nickel had a capacity of about 8 min 20 s, but the unused nickel ribbon produced negligible capacity.

Analysis of the electrolyte using atomic absorption spectroscopy before and after the experiment on samples taken from the counter electrode compartment revealed that the level of iron had increased from 1.4 to 2.1 ppm by the end of the

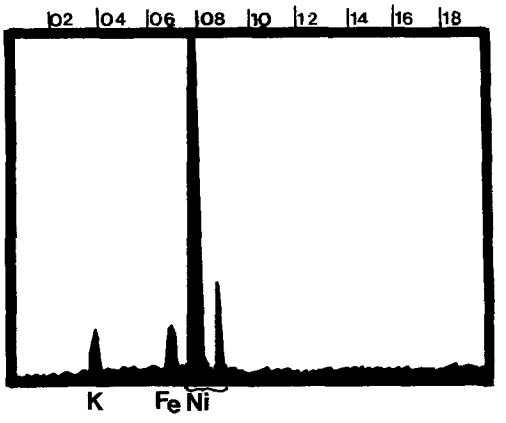

Fig. 4. EDAX Photograph, position A.

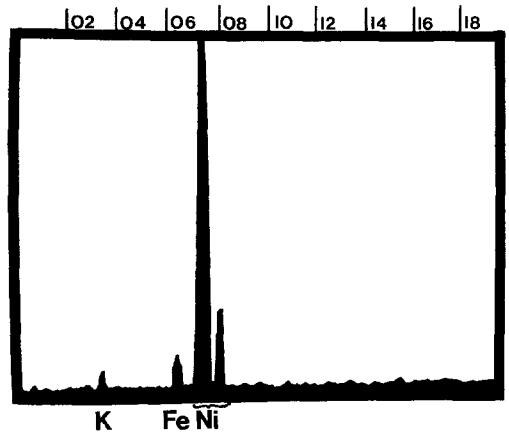

Fig. 5. EDAX Photograph, position B.

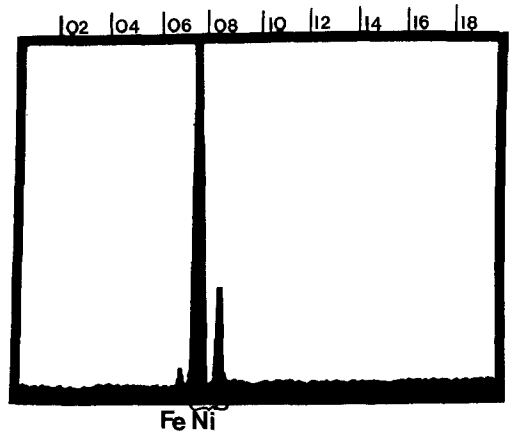

Fig. 6. EDAX Photograph, position C.

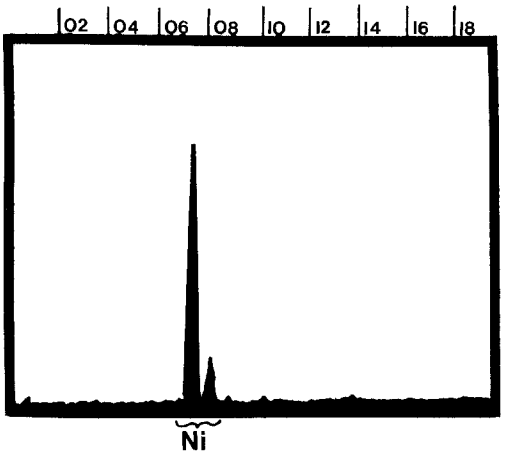

Fig. 7. EDAX photograph of the unused nickel.

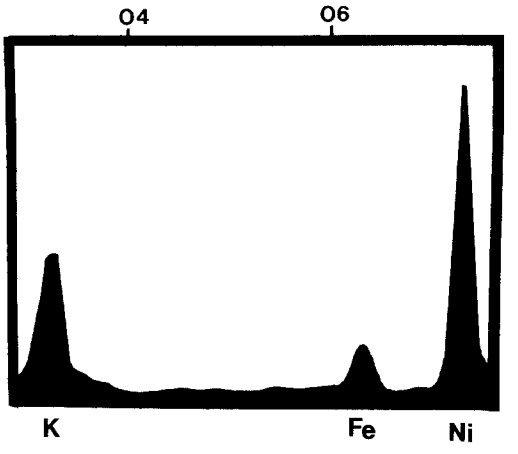

Fig. 9. EDAX Photograph of position B from the mild steel ribbon experiment.

experiment. The reproducibility of the low atomic absorption analysis for iron for such concentrations was found to be within 0.1 ppm over four samples.

In the experiment using the mild steel ribbon, a magnified EDAX photograph (Fig. 9) taken from position B of the nickel counter electrode again demonstrated the presence of iron. Coulometric analysis showed that at a constant current of 1 mA the capacity was 64 min (Fig. 10). Atomic absorption analysis of the electrolyte after the experiment showed an increase in the level of iron to 2.7 ppm.

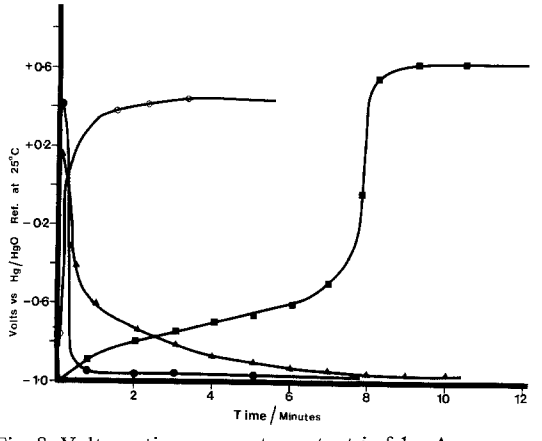

Fig. 8. Voltage–time curve at constant i of 1 mA. ■ discharge curve for used nickel, ▲ charge curve for used nickel, ○ discharge curve for unused nickel, ● charge curve for unused nickel.

3.2. *Cyclic voltammetric studies*

Fig. 11 shows a typical voltammogram for the nickel counter electrode with the electrodeposited material obtained from the experiment using the pure ribbon as the negative component. The potential was scanned between − 1.000 and − 0.0400 V (with reference to the Hg/HgO electrode). The general shape of the curves in both sets of experiments were very similar. Peaks I, II and III occur at − 837, − 755 and − 595 mV respectively. Only one reduction peak appears as expected, that at about − 860 mV.

As demonstrated by Ojefors [5] on the iron electrode, the processes occurring as shown in Fig. 11 are as follows:

$$\text{I} \quad \text{Fe} \rightarrow \text{HFeO}_2^- \rightarrow \text{Fe(OH)}_2 \qquad (1)$$

$$\text{II} \quad \text{Fe} \rightarrow \text{HFeO}_2^- \rightarrow \text{FeO}_2^- \rightarrow \text{FeOOH} \qquad (2)$$

$$\text{III} \quad \text{Fe(OH)}_2 \rightarrow \text{HFeO}_2^- \rightarrow \text{FeO}_2 \rightarrow \text{FeOOH} \qquad (3)$$

Process I occurs in the active (corrosion) potential region of iron and the first peak results from complete surface coverage with hydroxide, resulting in a partial passivation.

Process II occurs at potentials more positive (on the Hg/HgO scale) than about − 595 mV, when conversion of ferrous ions to ferric ions can take place. This results in a second sparingly soluble ion (FeO_2^-) which rapidly forms the solid FeOOH leading to the second, more complete, passivation. It is in this secondary passive region that steel lies

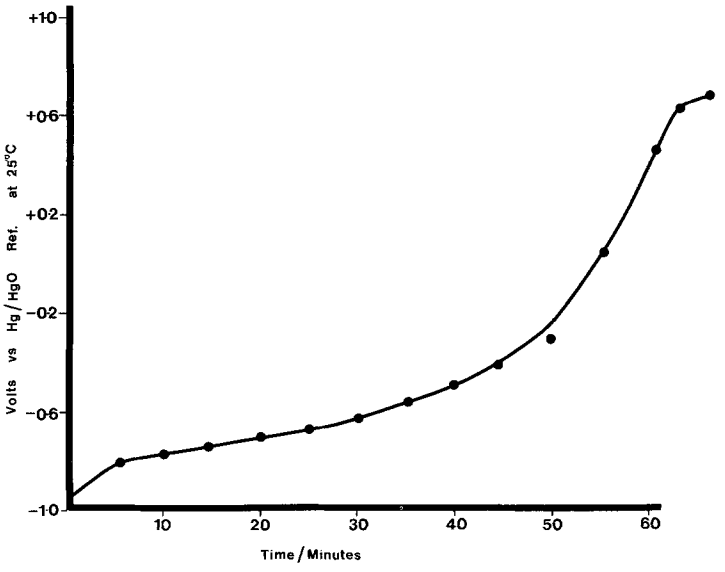

Fig. 10. Voltage–time curve at constant i of 1 mA. • Discharge curve for used nickel using the iron ribbon as the negative electrode.

in equilibrium in alkali, but when connected to a source of negative potential (e.g. cadium or a potentiostat), it lies in region I with the resulting tendency to corrode. By comparison, the unused pure nickel ribbon (Fig. 12) has very low electrochemical activity between − 0.400 and − 1.000 V vs Hg/HgO.

The voltages of these peaks coincide with the voltages expected for reactions I and III above and therefore the cyclic voltammetry results confirm that the deposit responsible for the coulometric capacity is iron. From observation of the potential and current scales it is seen that the iron peaks are readily distinguishable from that of nickel. The reasons for the relative stability of nickel in alkali are that the anodic current densities are lower than for iron and when connected to cadium (i.e. in a negative plate) or iron, nickel is negative to its reversible potential (− 817 mV) and is therefore cathodically protected under normal conditions.

The basic electrochemical reactions for iron and cadmium are as follows:

$$Cd(OH)_2 + 2e = Cd + 2OH^-$$
$$E^\circ = -0.809\ \text{V vs SHE} \qquad (4)$$
$$Fe(OH)_2 + 2e = Fe + 2OH^-$$
$$E^\circ = -0.877\ \text{V vs SHE} \qquad (5)$$

indicating that iron is cathodic to cadmium by about 70 mV.

These equations also indicate that 1 g of cadmium should give a capacity of 0.477 A h and 1 g of iron a capacity of 0.960 A h. Assuming that the reaction occuring is as above and that all of the iron oxide can be converted to iron, then a rough estimate of the amount of iron transferred over

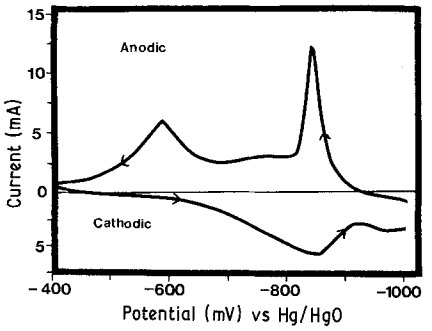

Fig. 11. Cyclic voltammetry for the used nickel ribbon in 5 M KOH, 300 m V min^{-1}.

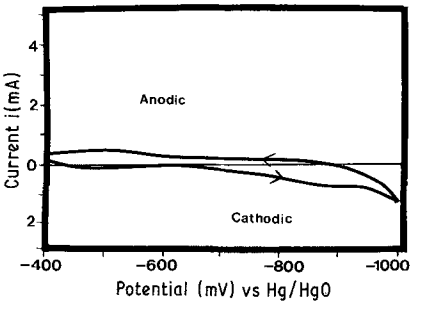

Fig. 12. Cyclic voltammetry for the used nickel ribbon in 5 M KOH, 300 m V min^{-1}.

Table 1. X-ray diffraction analysis of the active material, 5 M KOH at room temperature

State of active material	*Phases present*
As received	α-Fe_2O_3, β-$Cd(OH)_2$
	α-Fe_2O_3, α-$Fe_2O_3 \cdot H_2O$
Charged	α-Fe, γFe_2O_3, γ-$Fe_2O_3 \cdot H_2O$
	β-$Fe_2O_3 \cdot H_2O$, Cd, β-$Cd(OH)_2$
Discharged	α-$Fe_2O_3 \cdot H_2O$, γ-Fe_2O_3
	β-$Fe_2O_3 \cdot H_2O$, Cd, β-$Cd(OH)_2$

15 cycles is about 0.013% of the iron oxide. Over 2 000 cycles, as in the normal case of operation of a nickel–cadmium battery and assuming continuous transfer, this could increase to about 2% of the iron oxide. This figure is from the iron oxide alone, but if unplated steel ribbons are used to make the pockets, then the actual amount could increase by about 7–8 fold as shown by the cycling test.

3.3. *X-ray studies*

As it was difficult to get clear X-ray powder patterns using the diffractometer on the nickel ribbon, they were obtained on the active material in the charged and discharged state to elucidate any phase changes occuring during the electrolysis.

Table I shows the various phases present in the two states. The result indicates that during the cycling, the original α-Fe_2O_3 undergoes a structural change with the formation of various phases. The phases shown in the X-ray pattern include α-Fe_2O_3 and α-$Fe_2O_3 \cdot H_2O$. There is, however, no consistency as to the products formed during the charging and discharging modes and this is in agreement with the results of other researchers [4, 10]. The fact that γ-Fe_2O_3 and other forms of oxides are observed shows that part of all of the α-Fe_2O_3 must undergo reduction during the charging of the electrode to a lower state such as Fe and on oxidation it is this iron that dissolves, a minute fraction of it migrating to the nickel ribbon where it is deposited as iron.

4. Conclusions

The present study shows there is some dissolution of α-Fe_2O_3 and that iron can be deposited in other parts of the cell though the amount is likely to be very much lower than the amount dissolved from the perforated mild steel ribbons used to enclose the active material. However, for the complete elimination of iron deposition other nonferrous additives should be investigated.

Acknowledgement

This work was supported by the Science and Engineering Research Council (UK) and Marathon Alcad Limited.

References

[1] G. Troilius and G. Alfelt, 'Power Sources' Vol. 1, (edited by D. H. Collins) Pergamon, Oxford (1966). p. 377.
[2] G. M. Bulman and M. L. Green, private communication.
[3] M. Pourbaix, 'Atlas of Electrochemical Equilibria in Aqueous Solution', Pergamon Press, Oxford (1966).
[4] A. J. Salkind, S. U. Falk and G. J. Venutu, *J. Electrochem. Soc.* **111** (1964) 493.
[5] L. Ojefors, *ibid.* **123** (1976) 1139.
[6] A. J. Salkind and S. U. Falk, 'Alkaline Storage Batteries', Wiley, New York (1976) p. 631.
[7] R. L. Tichenor, *Ind. Eng. Chem.* **44** (1952) 973.
[8] D. Tuomi, *J. Electrochem. Soc.* **112** (1965) 1.
[9] J. Parker, private communication.
[10] H. G. Silver and E. Lakas, *J. Electrochem. Soc.* 117 (1970) 5.